# Aluminum plasmonic nanoparticles enhanced dye sensitized solar cells

**Qi Xu, Fang Liu,* Yuxiang Liu, Weisi Meng, Kaiyu Cui, Xue Feng, Wei Zhang, and Yidong Huang**

*Department of Electronic Engineering, Tsinghua National Laboratory for Information Science and Technology, Tsinghua University, Beijing 100084, China*
**liu_fang@mail.tsinghua.edu.cn*

**Abstract:** We present an investigation on utilizing plasmonic aluminium (Al) nanoparticles (NPs) to enhance the optical absorption of dye-sensitized solar cells (DSCs). The Al NPs exhibit not only the light absorption enhancement in solar cells with localized surface plasmon (LSP) effect but also the chemical stability to iodide/triiodide electrolyte. Besides, the lower work function (~4.06 eV), compared with that of $TiO_2$ (~4.6 eV), may suppress the quenching processes, such as charge transfer to metal NPs, to reduce the loss. Thus, high concentration of Al NPs could be incorporated into the $TiO_2$ anodes, and the power conversion efficiency (PCE) of DSCs is improved by nearly 13%. Moreover, electrochemical impedance spectroscopy (EIS) characterization also indicates that the plasmonic DSCs with Al NPs present better electrochemical performance than regular ones, which contributes to the improvement of PCE of the device.



**OCIS codes:** (040.5350) Photovoltaic; (250.5403) Plasmonics.

## References and links

1. B. O'regan and M. Grätzel, "A low-cost, high-efficiency solar cell based on dye-sensitized," Nature **353**, 24 (1991).
2. M. K. Nazeeruddin, A. Kay, I. Rodicio, R. Humphry-Baker, E. Müller, P. Liska, N. Vlachopoulos, and M. Grätzel, "Conversion of light to electricity by cis-X2bis (2, 2'-bipyridyl-4, 4'-dicarboxylate) ruthenium (II) charge-transfer sensitizers (X= Cl-, Br-, I-, CN-, and SCN-) on nanocrystalline titanium dioxide electrodes," J. Am. Chem. Soc. **115**(14), 6382–6390 (1993).
3. M. Grätzel, "Photoelectrochemical cells," Nature **414**(6861), 338–344 (2001).
4. M. Grätzel, "Dye-sensitized solar cells," J. Photochem. Photobiol. Photochem. Rev. **4**(2), 145–153 (2003).
5. E. Dulkeith, M. Ringler, T. A. Klar, J. Feldmann, A. Muñoz Javier, and W. J. Parak, "Gold nanoparticles quench fluorescence by phase induced radiative rate suppression," Nano Lett. **5**(4), 585–589 (2005).
6. M. Ihara, K. Tanaka, K. Sakaki, I. Honma, and K. Yamada, "Enhancement of the Absorption Coefficient of cis-(NCS) 2 Bis (2, 2'-bipyridyl-4, 4'-dicarboxylate) ruthenium (II) Dye in Dye-Sensitized Solar Cells by a Silver Island Film," J. Phys. Chem. B **101**(26), 5153–5157 (1997).
7. K. Ishikawa, C.-J. Wen, K. Yamada, and T. Okubo, "The photocurrent of dye-sensitized solar cells enhanced by the surface plasmon resonance," J. Chem. Eng. of Jpn **37**(5), 645–649 (2004).
8. C. Hagglund, M. Zach, and B. Kasemo, "Enhanced charge carrier generation in dye sensitized solar cells by nanoparticle plasmons," Appl. Phys. Lett. **92**, 013113 (2008).
9. S. D. Standridge, G. C. Schatz, and J. T. Hupp, "Toward plasmonic solar cells: protection of silver nanoparticles via atomic layer deposition of $TiO_2$," Langmuir **25**(5), 2596–2600 (2009).
10. C. Wen, K. Ishikawa, M. Kishima, and K. Yamada, "Effects of silver particles on the photovoltaic properties of dye-sensitized $TiO_2$ thin films," Sol. Energy Mater. Sol. Cells **61**(4), 339–351 (2000).
11. M. D. Brown, T. Suteewong, R. S. S. Kumar, V. D'Innocenzo, A. Petrozza, M. M. Lee, U. Wiesner, and H. J. Snaith, "Plasmonic dye-sensitized solar cells using core-shell metal-insulator nanoparticles," Nano Lett. **11**(2), 438–445 (2011).
12. J. Qi, X. Dang, P. T. Hammond, and A. M. Belcher, "Highly efficient plasmon-enhanced dye-sensitized solar cells through metal@oxide core-shell nanostructure," ACS Nano **5**(9), 7108–7116 (2011).
13. Q. Xu, F. Liu, W. Meng, and Y. Huang, "Plasmonic core-shell metal-organic nanoparticles enhanced dye-sensitized solar cells," Opt. Express **20**(S6), A898–A907 (2012).
14. X. Dang, J. Qi, M. T. Klug, P.-Y. Chen, D. S. Yun, N. X. Fang, P. T. Hammond, and A. M. Belcher, "Tunable Localized Surface Plasmon-Enabled Broadband Light-Harvesting Enhancement for High-Efficiency Panchromatic Dye-Sensitized Solar Cells," Nano Lett. **13**(2), 637–642 (2013).

#201517 - $15.00 USD Received 27 Nov 2013; revised 11 Jan 2014; accepted 12 Jan 2014; published 7 Feb 2014

15. Q. Xu, F. Liu, Y. Liu, K. Cui, X. Feng, W. Zhang, and Y. Huang, "Broadband light absorption enhancement in dye-sensitized solar cells with Au-Ag alloy popcorn nanoparticles," Sci. Rep. **3**, 2112 (2013).
16. S. D. Standridge, G. C. Schatz, and J. T. Hupp, "Distance dependence of plasmon-enhanced photocurrent in dye-sensitized solar cells," J. Am. Chem. Soc. **131**(24), 8407–8409 (2009).
17. G. Zhao, H. Kozuka, and T. Yoko, "Effects of the incorporation of silver and gold nanoparticles on the photoanodic properties of rose bengal sensitized $TiO_2$ film electrodes prepared by sol-gel method," Sol. Energy Mater. Sol. Cells **46**(3), 219–231 (1997).
18. W. M. Haynes, D. R. Lide, and T. J. Bruno, CRC Handbook of Chemistry and Physics 2012–2013, CRC press (2012).
19. V. Kochergin, L. Neely, C.-Y. Jao, and H. D. Robinson, "Aluminum plasmonic nanostructures for improved absorption in organic photovoltaic devices," Appl. Phys. Lett. **98**(13), 133305 (2011).
20. E. Stratakis, M. Barberoglou, C. Fotakis, G. Viau, C. Garcia, and G. A. Shafeev, "Generation of Al nanoparticles via ablation of bulk Al in liquids with short laser pulses," Opt. Express **17**(15), 12650–12659 (2009).
21. X. Chen, B. Jia, J. K. Saha, B. Cai, N. Stokes, Q. Qiao, Y. Wang, Z. Shi, and M. Gu, "Broadband enhancement in thin-film amorphous silicon solar cells enabled by nucleated silver nanoparticles," Nano Lett. **12**(5), 2187–2192 (2012).
22. P. K. Jain, X. Huang, I. H. El-Sayed, and M. A. El-Sayed, "Review of some interesting surface plasmon resonance-enhanced properties of noble metal nanoparticles and their applications to biosystems," Plasmonics **2**(3), 107–118 (2007).
23. A. V. Zayats, I. I. Smolyaninov, and A. A. Maradudin, "Nano-optics of surface plasmon polaritons," Phys. Rep. **408**(3-4), 131–314 (2005).
24. C. Nahm, H. Choi, J. Kim, D.-R. Jung, C. Kim, J. Moon, B. Lee, and B. Park, "The effects of 100 nm-diameter Au nanoparticles on dye-sensitized solar cells," Appl. Phys. Lett. **99**(25), 253107 (2011).
25. Q. Wang, J.-E. Moser, and M. Grätzel, "Electrochemical impedance spectroscopic analysis of dye-sensitized solar cells," J. Phys. Chem. B **109**(31), 14945–14953 (2005).
26. J. Bisquert, F. Fabregat-Santiago, I. Mora-Seró, G. Garcia-Belmonte, and S. Giménez, "Electron lifetime in dye-sensitized solar cells: theory and interpretation of measurements," J. Phys. Chem. C **113**(40), 17278–17290 (2009).
27. S. Chang, Q. Li, X. Xiao, K. Y. Wong, and T. Chen, "Enhancement of low energy sunlight harvesting in dye-sensitized solar cells using plasmonic gold nanorods," Energy Environ. Sci. **5**(11), 9444–9448 (2012).
28. H. Choi, W. T. Chen, and P. V. Kamat, "Know thy nano neighbor. Plasmonic versus electron charging effects of metal nanoparticles in dye-sensitized solar cells," ACS Nano **6**(5), 4418–4427 (2012).

## 1. Introduction

Dye-sensitized solar cells (DSCs) have attracted increasing interest due to their relatively high efficiency and low cost of component materials in recent years [1–4]. However, limited by the poor light harvesting in thin photoanodes, the power conversion efficiency (PCE) of DSCs is hard to be improved significantly [5]. Recently, the plasmonic nanoparticles (NPs) have been incorporated into the photoanodes of DSCs to utilize their localized surface plasmon (LSP) light trapping effect to significantly boost the light absorption of dye molecules and consequently the PCE of devices [6–10]. Gold and silver plasmonic NPs and their core-shell nanostructures have been employed in DSCs to improve the properties of solar cell by the LSP enhanced light absorption [11–14]. It is also indicated that the optical absorption of the DSCs could be further improved if the concentration of the plasmonic NPs incorporated are increased [15]. However, for Ag or Au NPs, limited by the quenching process of carriers, it is difficult to increase the concentration of metal NPs for further making use of the LSP light trapping effect [16,17]. If the quenching process of the metal NPs could be suppressed, more plasmonic NPs could be incorporated into the DSCs and it is anticipated that a more significant efficiency improvement of DSCs with LSP effect can be obtained.

Here, the plasmonic aluminium (Al) NPs enhanced DSCs is proposed and investigated. Compared with Au or Ag, the Al NPs has the same LSP enhanced light absorption, but better chemical stability to iodide/triiodide electrolyte and elower work function (~4.06 eV), even lower than the conduction band of $TiO_2$ (~4.6 eV) [18], which could suppress the quenching process and reduce the loss induced by charge transfer to metal NPs. The experimental results show that, with no significant worsening of carrier transportation of anode, the concentration of Al NPs incorporated into DSCs can be greatly increased, which is also confirmed by the electrochemical impedance measurement of Al NPs enhanced DSCs. The PCE of plasmonic DSCs incorporated with Al NPs is improved from 6.15% to 6.95% with nearly 13% enhancement. The optimized density of Al NPs, which corresponds to the highest PCE enhancement of DSCs, is about 8 times higher than that of Au NPs. Although the light

#201517 - $15.00 USD Received 27 Nov 2013; revised 11 Jan 2014; accepted 12 Jan 2014; published 7 Feb 2014

trapping effect of Al NPs is not as good as that of Au or Ag with the same nanoparticle density [19], the suppressed quenching process provides the possibility of incorporating more metal NPs into DSCs. Thus it is possible to improve PCE further if some kinds of novel metal NPs, such as Au or Ag NPs coated with an Al shell, are utilized.

## 2. Result and discussion

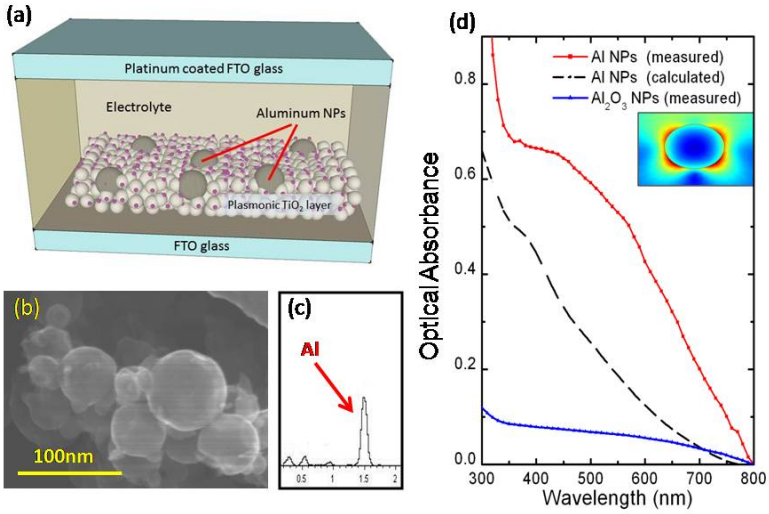


Fig. 1. (a) Schematic structure of plasmonic Aluminum (Al) nanoparticles (NPs) enhanced dye-sensitized solar cells (DSCs). (b) Scanning electron microscopy (SEM) image of Al NPs. (c) Energy dispersive spectroscopy (EDS) measurement result of Al NPs. (d) Calculated optical absorption of Al NPs (black curve) and measured optical absorption of Al NPs (red curve) and $Al_2O_3$ NPs (blue curve) in ethanol solutions. The concentrations of Al NPs and $Al_2O_3$ NPs are the same. Inset: The calculated LSP field distribution of the 50nm Al NP illuminated by incident light at wavelengths of 380 nm.

Figure 1(a) shows the schematic structure of plasmonic-enhanced DSCs incorporated with Al NPs. The Al NPs (purchased from Aladin, 99.99% purity) are embedded in the mesoporous $TiO_2$ layer, which would help to improve the optical absorption of dye molecules via the LSP induced light-trapping effect. To get rid of the oxidization shell which might form on the surface of the commercial Al NPs, we use 0.1% hydrochloric acid (HCl) to wash the Al NPs for 5-6 min. The scanning electron microscopy (SEM, HITACHI S-5500, 30kV) image of the Al NPs after treated is shown in Fig. 1(b). It can be observed that the average diameter of the Al NPs is about 50nm. The spectrum of energy dispersive spectroscopy (EDS, Horiba EX-250) shown in Fig. 1(c) also indicates the dominant element of the NPs is aluminium. The other peaks in the EDS spectrum correspond to C, H, and Cu element which come from the carrier and clamp used in SEM measurement. The measurement results of optical absorption spectroscopy (U-3010, HITACHI) show that, the Al NPs exhibit a wide LSP absorption "shoulder" between 350 and 450 nm, as shown by red square line in Fig. 1(d), which is consistent with the calculated curve (black dashed line) and the earlier literatures [20]. To be noticed, it also exhibits an absorption 'tail' from 500 to 700nm, which is supposed to be the scattering effect of Al NPs [21,22].

To clarify the role of plasmonic and scattering effect, the optical absorption measurement of 50nm $Al_2O_3$ NPs (purchased from Aladin, 99.5% purity) is also carried out to compare with the light absorption of Al NPs. With the same concentration of Al NPs and $Al_2O_3$ NPs in

#201517 - $15.00 USD Received 27 Nov 2013; revised 11 Jan 2014; accepted 12 Jan 2014; published 7 Feb 2014

ethanol, the solution with Al NPs exhibit much stronger optical absorption especially in the short wavelength range. Since the $Al_2O_3$ NPs do not possess plasmonic effect, the LSP effect should play a primary role in the optical absorption of the Al NPs. Besides, the calculated electrical field distribution (Inset in Fig. 1(d)) also indicates that the Al NPs of 50nm support higher order LSP modes (See *Appendix*) [23].

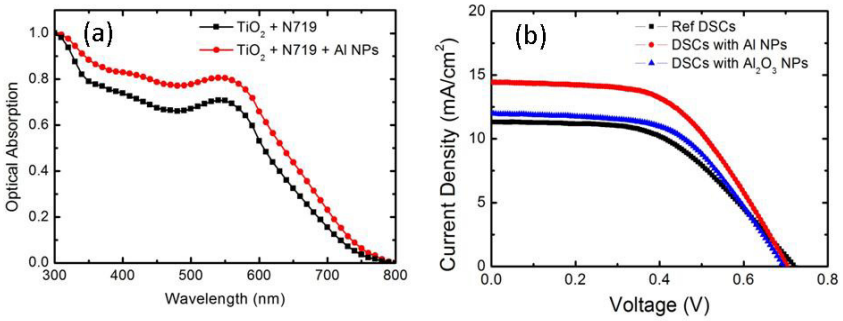


Fig. 2. (a) Optical Absorption of dye-sensitized $TiO_2$ anodes incorporated with/without Al NPs. (b) The photocurrent density-voltage characteristics (J-V curves) of DSCs incorporated with Al or $Al_2O_3$ NPs and $TiO_2$-only DSCs. The $TiO_2$ anodes are composed of 3μm active layers (25nm $TiO_2$ NPs).

To investigate the plasmonic effect of Al NPs in $TiO_2$ layers and DSCs, the plasmonic $TiO_2$ anodes incorporated with Al NPs are fabricated by spin-coating method [12] (See *Appendix*). The thickness of the $TiO_2$ layers are set to be 3μm, which is much thinner than typical ones for the purpose of clarifying the effects caused by Al nanoparticles as mentioned by Ref [24]. For comparison of light trapping effect, the $TiO_2$–only photoanode and $TiO_2$ photoanode incorporated with $Al_2O_3$ NPs are also prepared by mixing the $TiO_2$ paste with ethanol or $Al_2O_3$ NPs in the same proportion of Al NPs.

Figure 2(a) shows the optical absorption of dye-sensitized $TiO_2$ anodes incorporated with/without Al NPs. Obvious optical absorption enhancement could be observed in plasmonic DSCs, which is supposed to be resulted from the LSP effect of Al NPs. To make further investigations, the plasmonic DSCs are fabricated based on the above anodes. Figure 2(b) shows the current density versus voltage characteristics (J-V curves) of $TiO_2$-only DSCs and DSCs incorporated with Al and $Al_2O_3$ NPs. It is clear that the short-circuit current density (Jsc) of the DSCs with Al NPs are increased significantly compared with the reference one, which results from the LSP light trapping effect of the Al NPs. On the other hand, the DSCs with $Al_2O_3$ NPs also have a tiny improvement on $J_{sc}$ which should be related to the scattering effect, but it is much lower than that induced by Al NPs with LSP effect. Compared with non-plasmonic $Al_2O_3$ NPs of the similar sizes, the device with Al NPs present a much higher photocurrent, which is result from the LSP near-field light trapping effect. Even if there is parasitic loss inside the Al NPs, the performance is still improved due to the LSP light trapping of the Al NPs.

**Table 1. Performance of DSCs composed of 8μm active layers and 2μm scattering layers.**

| *Device* | *Composition* | *$V_{oc}$ (V)* | *$J_{sc}$ (mA/cm$^2$)* | *FF (%)* | *PCE (%)* |
|---|---|---|---|---|---|
| 1 | $TiO_2$-only | 0.716 ± 0.05 | 15.18 ± 0.02 | 56.6 ± 0.1 | 6.15 ± 0.1 |
| 2 | 0.25 wt % Al NPs | 0.719 ± 0.09 | 15.39 ± 0.04 | 56.1 ± 0.2 | 6.25 ± 0.1 |
| 3 | 0.75 wt % Al NPs | 0.720 ± 0.08 | 17.61 ± 0.03 | 56.3 ± 0.2 | 6.95 ± 0.1 |
| 4 | 1.50 wt % Al NPs | 0.721 ± 0.10 | 15.37 ± 0.02 | 57.5 ± 0.1 | 6.36 ± 0.1 |
| 5 | 7.5 wt% Al NPs | 0.717 ± 0.11 | 14.64 ± 0.02 | 55.9 ± 0.3 | 5.88 ± 0.1 |

#201517 - $15.00 USD Received 27 Nov 2013; revised 11 Jan 2014; accepted 12 Jan 2014; published 7 Feb 2014

To obtain the optimized performance of the DSCs, we fabricate thick $TiO_2$ anodes composed of 8μm active layers (25nm $TiO_2$ NPs) and 2μm scattering layers (200 nm $TiO_2$ NPs) by utilizing doctor-blading method [14]. The performance of DSCs with different amount of Al NPs is shown in Table 1. It is clearly demonstrated that there is a maximum enhancement in both the $J_{sc}$ and PCE of the DSCs incorporated with certain concentrations of Al NPs (0.75 wt% for device 3), and both lower and higher concentration (0.25 wt% for device 2, 1.5 wt% for device 4 and 7.5 wt% for device 5) lead to reduction of PCE compared with that of device 3. The PCE of the plasmonic DSC with 0.75 wt% Al NPs (device 3) reaches 6.95%, which indicates an enhancement of nearly 13% compared with that of the reference DSC (device 1). The J-V curves are shown in Fig. 3(a). The $V_{oc}$ and fill factors (FF) remain nearly unchanged, while the $J_{sc}$ shows an obvious increase due to the LSP-enhanced optical absorption of the dye molecules.

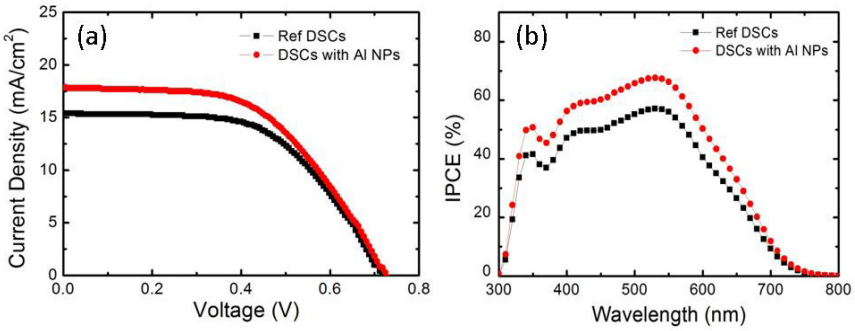


Fig. 3. (a) The J-V curves of DSCs incorporated with Al NPs at optimised concentration of 0.75 wt% and $TiO_2$-only DSCs, the $TiO_2$ anodes are composed of 8μm active layers (25nm $TiO_2$ NPs) and 2μm scattering layers (200 nm $TiO_2$ NPs). (b) Incident photon-to-electron conversion efficiency (IPCE) of Al NPs enhanced DSCs and $TiO_2$-only DSCs.

The incident photon-to-electron conversion efficiency (IPCE) (QEX10, PV Measurement, USA) of Al NPs enhanced DSCs and $TiO_2$-only DSCs are shown in Fig. 3(b). It is indicated that the IPCE of the Al NPs enhanced DSCs is improved over a wide wavelength range from about 350 to 650nm similar to the optical absorption enhancement in Fig. 2(a), which should be attributed to the light harvesting enhancement induced by LSP effect. Compared with the LSP absorption between 350 and 450nm in Fig. 1(d), there is a red shift for the LSP enhancement in $TiO_2$ films, which would mainly result from the increase of refractive index of the surrounding materials [23]. To be noticed, although the scattering effect of the Al NPs contributes to the enhancement, the plasmonic effect still dominates because of the relatively small size of the NPs.

What should be mentioned is that here the nanoparticle density ($D_{NPs}$) of Al NPs in the $TiO_2$ layers, namely the number of NPs per unit volume, is much higher than that of Au or Au NPs in previous works [12] (See *Appendix*). The concentration of metal NPs is often defined by mass concentration (as shown in Table 1) [13–15]. However, it could not clearly reflect the DNPs, which is related to the loss of quenching process of carriers induced by the metal NPs [24]. When DNPs is increased, the rate of the quenching reaction would rise, leading to the decline of Jsc and PCE of the DSCs.

Here, the optimized mass concentration of Al NPs is 0.75 wt%, which is similar to that of Au/Ag NPs reported by other groups [12,25]. However, due to the difference of their mass density ρmetal, the $D_{NPs}$ of Al NPs is about 8 (4) times higher than that of Au (Ag) NPs. It is amazing that such a high DNPs doesn't lead to high loss of carriers because the quenching reactions in $TiO_2$ layer is suppressed and the PCE is well improved, different from e Ag/Au NPs [12,25]. This result indicates that the Al NPs would cause much less loss of carriers, induced by quenching process in $TiO_2$ layer, than Au or Ag NPs. Moreover, even the concentration of Al NPs is set to be 10 times higher than the optimized one (device 5 in Table 1), the $J_{sc}$ and PCE of the device still present considerable values.

#201517 - $15.00 USD Received 27 Nov 2013; revised 11 Jan 2014; accepted 12 Jan 2014; published 7 Feb 2014

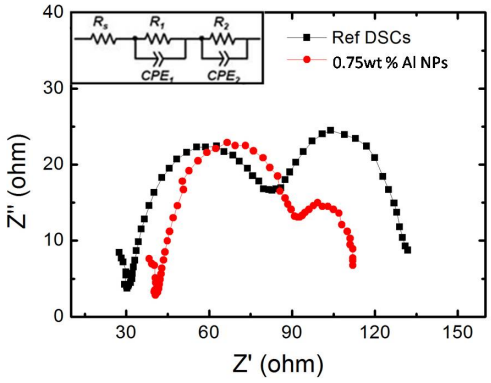


Fig. 4. Electrochemical impedance spectra (EIS) of DSCs incorporated with/without Al NPs. Inset is the equivalent circuit.

To gain further insight into the reactions between different components of the device, the electrochemical impedance spectra (EIS) are measured. The EIS curves and properties of DSCs with (device 2, 3 and 4) and without (device 1) Al NPs are shown in Fig. 4 and Table 2, respectively, where $R_2$, $R_l$, and $R_s$ represent the impedance related to the electron transport in the $TiO_2$/dye/electrolyte interface, the charge transfer at the platinum counter electrode, and the sheet resistance of the FTO, respectively [26]. In EIS spectrum, the increased Rs is due to the incorporation of Al NPs and their negative affection to FTO electrode. However, $R_2$ decreases when increasing the concentration of Al NPs till the optimized value of 0.75 wt %, which means that the electron transport efficiency in the $TiO_2$/dye/electrolyte interface is improved. This phenomenon is unusual because other metal NPs such as Au or Ag perform inversely [27]. The peak frequency of the second semi-circle fmax for reference DSCs is 11.91 Hz, while for the optimized plasmonic DSCs with 0.75 wt% Al NPs it reduces to 8.07 Hz (as shown in Table 2). The electron lifetime τ inversely associated with $f_{max}$ ($f_{max} = 1/\tau$) is 0.124 s for Al NPs enhanced DSCs [25], which is longer than the reference DSCs (0.084s of device a, Table 2) and contributes to the improvement of PCE.

**Table 2. Electrochemical impedance spectra (EIS) properties of DSCs incorporated with/without Al NPs.**

| *Device* | *Composition* | *$R_s$ (Ω)* | *$R_2$ (Ω)* | *$f_{max}$ (Hz)* | *τ (s)* |
|---|---|---|---|---|---|
| 1 | $TiO_2$-only | 28.59 | 62.98 | 11.91 | 0.084 |
| 2 | 0.25 wt % Al NPs | 31.25 | 53.95 | 10.79 | 0.093 |
| 3 | 0.75 wt % Al NPs | 33.52 | 27.89 | 8.07 | 0.124 |
| 4 | 1.50 wt % Al NPs | 35.53 | 47.79 | 9.89 | 0.101 |

The unusual phenomenon mentioned above could be understood according to the following analysis. The work function of metal Au (5.47 eV) and Ag (4.74 eV) is larger than that of $TiO_2$ (~4.6 eV) [18]. The photon generated electrons in the conduction band of $TiO_2$ would tend to transfer to the Au or Ag NPs with lower potential [28], leading to quenching reactions and hamper the photocurrent and the PCE of the device. That is why Au or Ag NPs could easily become the recombination centres. Nevertheless, Al possesses lower work function (~4.06 eV) than that of $TiO_2$ (~4.6 eV), which means the potential of Al is higher than that of $TiO_2$. The higher potential of Al NPs may reduce the loss resulting from charge transfer to metal NPs and suppress the quenching processes. Therefore, the reasons for lower R2 of DSCs with Al NPs can be concluded as follows: First, more carriers are generated due to the LSP based light harvesting effect of Al NPs, as indicated by the longer electron lifetime τ; secondly, the higher potential of Al NPs hampers the carrier transfer from $TiO_2$ to metal

#201517 - $15.00 USD Received 27 Nov 2013; revised 11 Jan 2014; accepted 12 Jan 2014; published 7 Feb 2014

NPs and reduces the loss induced by quenching process significantly. These two reasons make the DSCs represent better performance on electrochemical impedance, as reflected by $R_2$. To be mentioned, the $R_2$ increases when the concentration of Al NPs is higher than the optimized value, which can be explained that excessive Al NPs will take too much places of $TiO_2$ NPs to reduce the amount of sensitized dye molecules.

What should be noticed is that, besides the quenching process, parasitic absorption loss inside the Al NPs also exists, which acts as a negative effect to hamper the performance. When the concentration of Al NPs rises, the overall losses from both quenching process and parasitic absorption will increase, resulting in the degradation of the device. The lower work function of Al NPs leading to the suppression of quenching process may compensate these losses, whilst the optical absorption of dye molecules will be significantly improved due to the LSP light trapping and scattering effect, which ensures the photocurrent and PCE of the device is well improved.

For improving the light trapping of DSCs, the Al NPs is not as good as Au or Ag, due to the larger energy loss of LSP mode. However, the Al NPs exhibit the advantage in reducing the quenching loss, which enable us to incorporate more metal NPs with LSP effect in $TiO_2$ layer. Therefore, it provides the possibility of further improving the PCE of DSCs by incorporating more plasmonic NPs with strong LSP effect, if novel metal NPs, such as Au-Al core-shell NPs, are realized.

## 3. Conclusion

In summary, plasmonic Al NPs enhanced DSCs is proposed and investigated. The plasmonic effect of Al NPs and the electrochemical impedance spectra of DSCs with Al NPs are studied. By incorporating Al NPs of different concentrations, a nearly 13% enhancement of PCE is obtained by optimizing the concentration of Al NPs. It is demonstrated that the nanoparticle density of Al NPs incorporated in $TiO_2$ layer is much higher than that of Au or Ag NPs. The electrochemical characterization results indicate that the Al NPs could suppress the quenching process and reduce the loss of carriers induced by metal NPs. This provides the possibility of further improving the PCE of DSCs by incorporating novel plasmonic NPs with both suppressed quenching process and strong LSP effect.

## Appendix

### 1. Methods

*Numerical calculations*

Instead of 3D model, 2D model based on the finite element method (FEM) is established for simplicity. In this study, the COMSOL software program (RF Module, COMSOL Multiphysics 3.5a) adopting the FEM to solve the Maxwell equations is applied to calculate the LSP modes supported by a Al NP at different wavelengths. The Al NP is located in a rectangular area (900 nm×900 nm) with side and bottom boundaries both set as absorbing boundaries. The optical properties of Al, including the wavelength-dependent refractive index $n$ and extinction coefficient $k$, are obtained from the literature [18]. A plane wave with wavelength $\lambda_0$ is set to simulate the incident light. Varying $\lambda_0$, LSP modes at different wavelengths are demonstrated.

*Fabrication of DSCs*

To fabricate the plasmonic $TiO_2$ anodes, spin-coating method and doctor-blading method are used for thin and thick $TiO_2$ layers, respectively. Briefly, 0.2 g $TiO_2$ paste (P25, Dyesol) is dispersed in 2.5 mL ethanol for spin-coating methods or in 0.2 mL for doctor-blading method, and then mixed with an Al NP ethanol solution, followed by sonicating for 10 min. The ratio of Al NPs to $TiO_2$ could be readily adjusted by changing the concentration of NPs in solution. To fabricate the thin $TiO_2$ layer, the plasmonic $TiO_2$ paste is spin-coated on a FTO glass substrate at 1800 rpm for 30 seconds to form a 3μm $TiO_2$ anode. Doctor-blading system is used to produce thick $TiO_2$ anodes. 8μm active layers composed of 25nm $TiO_2$ NPs (P25,

#201517 - $15.00 USD Received 27 Nov 2013; revised 11 Jan 2014; accepted 12 Jan 2014; published 7 Feb 2014

Dyesol) and 2um scattering layers composed of 200 nm $TiO_2$ NPs (P200, Dyesol) are printed onto the FTO glass. Then, the $TiO_2$ photoanodes are annealed at 500°C for 30 min. $TiO_2$–only photoanode or $TiO_2$ photoanode incorporated $Al_2O_3$ NPs are also prepared by mixing the $TiO_2$ paste with ethanol or $Al_2O_3$ NPs in the same proportion for comparison. The thickness of both the $TiO_2$–only and plasmonic $TiO_2$ layer are measured using a Dektak 150 surface profiler. These photoanodes are immersed in a 0.1 mM dye (N719, purchased form Dyesol) ethanol solution and kept at room temperature for 18 h. Then, the impregnated photoanodes are placed in ethanol for 5 min to remove the non-adsorbed dye, followed by natural drying in air. Finally, the device is sealed by a sealing frame (Surlyn sealant) and injected with electrolyte (EL-HPE, Dyesol). The electrolyte mainly consisted of $I_2$ and LiI in an acetonitrile solvent.

*Photovoltaic characterisation of DSCs*

The current-voltage characteristics of DSCs are measured under AM 1.5G illumination using a solar simulator (XEC-300M2, SAN-EI, Japan). The power of the simulated light is calibrated to 1,000 W/m$^2$ using a standard reference Si solar cell, and I-V curves are obtained by applying an external bias to the cell and measuring the generated photocurrent with a digital source meter (KEITHLEY 2400, USA). The voltage step and delay time of the photocurrent are 6 mV and 30 ms, respectively. To investigate the light absorption enhancement based on the LSP effect at different wavelengths, the spectral response of the solar cells is observed by using an IPCE measurement system (QEX10, PV Measurement, USA) consisting of a 150 W xenon lamp light source. The incident photon flux is also determined by using a calibrated silicon photodiode.

*Electrochemical characterisation of DSCs*

Electrochemical impedance spectra (EIS) is measured over a frequency range of 0.1 to 10000 Hz with an AC amplitude of 5 mV by using the electrochemical workstation (CHI 604A). The initial potential is set to be –0.65V and the quiet time is 2 sec. The properties are calculated from Z-View software (v2.1b, Scribner Associate, Inc).

**2. Chemical stabilities of Al NPs**

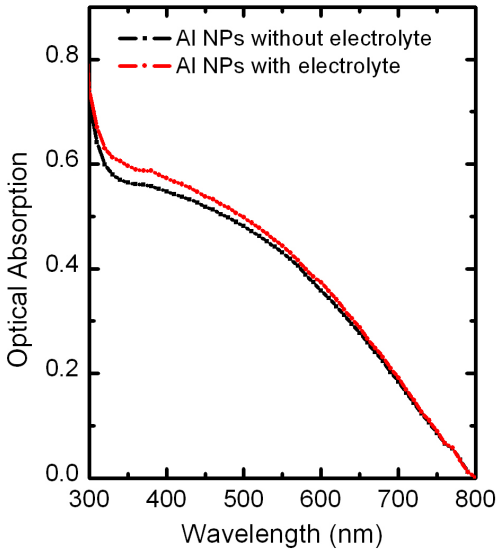


Fig. 5. Optical absorption of Al NPs in ethanol solution before/after being mixed with electrolyte.

#201517 - $15.00 USD Received 27 Nov 2013; revised 11 Jan 2014; accepted 12 Jan 2014; published 7 Feb 2014

Figure 5 shows the optical absorption of Al NPs in ethanol solution before (black curve) and after (red curve) being mixed with iodide/triiodide redox couple-based electrolyte. The LSP absorption 'shoulder' occurs at about 400nm did not disappear when mixed with electrolyte, which demonstrates that the Al NPs did not react with the electrolyte. It is different from Au or Ag NPs that we don't need to form a protective shell at the surface of the NPs.

### 3. Calculated LSP field distribution of Al NPs

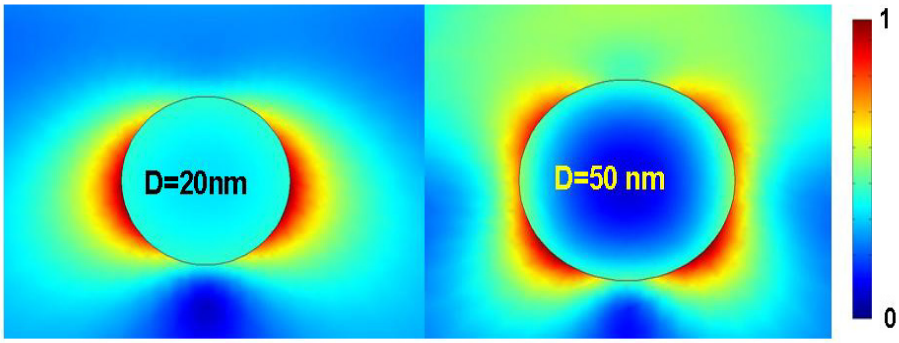


Fig. 6. The calculated LSP field distribution of the Al NP with the diameter D of 20nm (left) and 50nm (right) which is illuminated by incident light at wavelengths of 360 nm (left) and 350nm (right).

Figure 6 shows the distribution of the norm of the electrical field $|E|$ of an Al NPs in the $TiO_2$ layer with an incident plane wave. The colour bar shows the intensity normalised by the maximum value. From the calculated result, we can see that for small Al NPs such as $D$ = 20nm, the trapped electrical field surrounding Al NPs belongs to first-order LSP mode (left figure in Fig. 6), while as the diameter of the NP increase, higher-order mode is excited (right figure in Fig. 6) [23].

### 4. Analysis on concentrations of plasmonic NPs

The concentration of incorporated Al NPs is defined by mass fraction $\frac{m_{NPs}}{m_{TiO_2}}$, where $m_{\mathrm{NPs}}$ and $m_{\mathrm{TiO2}}$ are the mass of metal NPs and $TiO_2$ layer, respectively. However, it could not clearly reflect the density of NPs distributed in $TiO_2$ layer since the densities of metal materials, such as Al, Au and Ag, are different. Assuming that the NPs are distributed uniformly, here we define the density of NPs $D_{\mathrm{NPs}}$, which is the number of plasmonic NPs distributed in unit volume of mesoporous $TiO_2$, to reflect how many metal NPs are incorporated into the solar cells. The rate of quenching reaction between metal NPs and photon carriers should be related with $D_{\mathrm{NPs}}$. When $D_{\mathrm{NPs}}$ is increased, the recombination probability would rise, leading to the decline of $J_{\mathrm{sc}}$ and PCE of the DSCs.

The density of NPs $D_{\mathrm{NPs}}$ can be express as follows:

$$D_{NPs} = \frac{N_{NPs}}{V_{TiO_2}} = \frac{m_{NPs}}{m_{NP} \times V_{TiO_2}} = \frac{m_{NPs} \times \rho_{TiO_2}}{V_{NP} \times \rho_{metal} \times V_{TiO_2} \times \rho_{TiO_2}} = \frac{\rho_{TiO_2}}{V_{NP} \times \rho_{metal}} \times \frac{m_{NPs}}{m_{TiO_2}} \quad (1)$$

where $N_{\mathrm{NPS}}$ is the total number of metal NPs, $V_{\mathrm{TiO2}}$ is the volume of $TiO_2$ layer, $m_{\mathrm{NPs}}$ is the total mass of metal NPs, $m_{\mathrm{NP}}$ is the average mass of singe metal NP, $V_{\mathrm{NP}}$ is the average volume of single metal NP, $\rho_{\mathrm{metal}}$ is the density of the metal NPs, $\rho_{\mathrm{TiO2}}$ is the equivalent density of $TiO_2$ layer and $m_{\mathrm{TiO2}}$ is the mass of $TiO_2$ layer. Since $\rho_{\mathrm{TiO2}}$ is unchanged for a certain $TiO_2$ layer, when $V_{NP}$ and $\frac{m_{NPs}}{m_{TiO_2}}$ are fixed, $D_{\mathrm{NPs}}$ would change inversely with $\rho_{\mathrm{metal}}$.

#201517 - $15.00 USD Received 27 Nov 2013; revised 11 Jan 2014; accepted 12 Jan 2014; published 7 Feb 2014

Therefore, the $D_{NPs}$ of Al NPs would be approximately 8 times that of Au NPs for the $\rho_{metal}$ of Al is about 1/8 of that of Au

**Acknowledgments**

This work was supported by the National Basic Research Programs of China (973 Program) under Contracts No. 2013CBA01704, 2010CB327405 and 2011CBA00608; the National High-tech R&D Program (863 Program) under Contract No. 2011AA050504; and the National Natural Science Foundation of China (NSFC-61036011, NSFC-61107050, and NSFC-61036010).

#201517 - $15.00 USD Received 27 Nov 2013; revised 11 Jan 2014; accepted 12 Jan 2014; published 7 Feb 2014